THE JOURNAL OF BIOLOGICAL CHEMISTRY VOL. 283, NO. 31, pp. 21579–21587, August 1, 2008

ATP Modulation of Ca^{2+} Release by Type-2 and Type-3 Inositol (1, 4, 5)-Triphosphate Receptors

*DIFFERING ATP SENSITIVITIES AND MOLECULAR DETERMINANTS OF ACTION**

Received for publication, February 29, 2008, and in revised form, April 18, 2008 Published, JBC Papers in Press, May 27, 2008, DOI 10.1074/jbc.M801680200

Matthew J. Betzenhauser[‡1], Larry E. Wagner II[‡], Miwako Iwai[§], Takayuki Michikawa[¶], Katsuhiko Mikoshiba[¶], and David I. Yule[‡2]

From the [‡]Department of Pharmacology and Physiology, School of Medicine and Dentistry, University of Rochester Medical Center, Rochester, New York, the [§]Division of Molecular Neurobiology, Department of Basic Medical Sciences, Institute of Medical Science, University of Tokyo, Tokyo, Japan, and the [¶]Laboratory for Developmental Neurobiology, Brain Development Research Group, Brain Science Institute, RIKEN, Saitama, Japan

ATP enhances Ca^{2+} release from inositol (1,4,5)-trisphosphate receptors ($InsP_3R$). However, the three isoforms of $InsP_3R$ are reported to respond to ATP with differing sensitivities. Ca^{2+} release through $InsP_3R1$ is positively regulated at lower ATP concentrations than $InsP_3R3$, and $InsP_3R2$ has been reported to be insensitive to ATP modulation. We have reexamined these differences by studying the effects of ATP on $InsP_3R2$ and $InsP_3R3$ expressed in isolation on a null background in DT40 $InsP_3R$ knockout cells. We report that the Ca^{2+}-releasing activity as well as the single channel open probability of $InsP_3R2$ was enhanced by ATP, but only at submaximal $InsP_3$ levels. Further, $InsP_3R2$ was more sensitive to ATP modulation than $InsP_3R3$ under similar experimental conditions. Mutations in the ATPB sites of $InsP_3R2$ and $InsP_3R3$ were generated, and the functional consequences of these mutations were tested. Surprisingly, mutation of the ATPB site in $InsP_3R3$ had no effect on ATP modulation, suggesting an additional locus for the effects of ATP on this isoform. In contrast, ablation of the ATPB site of $InsP_3R2$ eliminated the enhancing effects of ATP. Furthermore, this mutation had profound effects on the patterns of intracellular calcium signals, providing evidence for the physiological significance of ATP binding to $InsP_3R2$.

The inositol (1,4,5)-trisphosphate ($InsP_3$)[3] receptors ($InsP_3R$) are a family of large tetrameric cation channels composed of four ~300-kDa subunits primarily localized to the endoplasmic reticulum. $InsP_3R$ act as $InsP_3$-gated channels that release Ca^{2+} from endoplasmic reticulum stores into the cytosol upon activation (1). In mammals, three distinct gene products plus additional splice variants code for three $InsP_3R$ isoforms ($InsP_3R1$, $InsP_3R2$, and $InsP_3R3$) (2–6). Sequence diversity, especially in the regions outside the conserved NH_2-terminal $InsP_3$-binding and COOH-terminal channel-forming domains, probably results in differential modulation of the three $InsP_3R$ isoforms by cellular factors, including Ca^{2+}, ATP, protein kinases, and binding proteins (7–9). Isoform-specific modulation by these factors may partially account for the complex spatial and temporal diversity of intracellular Ca^{2+} signals displayed by mammalian cells.

ATP enhances $InsP_3$-mediated Ca^{2+} release from endoplasmic reticulum stores in a variety of cell types expressing mixed or homogenous $InsP_3R$ populations (10–13). Consistent with these observations, ATP also increases the open probability of single $InsP_3R1$ and $InsP_3R3$ channels in lipid bilayers as well as in nuclear patches (14–17). Importantly, this form of modulation does not require hydrolysis, since nonhydrolyzable ATP analogues enhance $InsP_3R$ activity to the same extent as ATP (10, 14). Analysis of endogenous *Xenopus* $InsP_3R$ or recombinant rat $InsP_3R3$ in *Xenopus* oocyte nuclear patches has established that ATP acts as an allosteric modulator primarily by enhancing $InsP_3R$ stimulation by Ca^{2+} (8, 16, 17).

Few studies have compared, in isolation, the effects of ATP on the three $InsP_3R$ isoforms under identical experimental conditions (13, 15). The limited data suggest that the relative sensitivity to ATP differs among the three isoforms, with $InsP_3R1$ activity being enhanced by micromolar [ATP] and $InsP_3R3$ being augmented by millimolar [ATP] (15). Interestingly, $InsP_3R2$ was shown to be functionally insensitive to ATP modulation in Ca^{2+} release assays as well as in single channel measurements (13, 15). The observed differences in sensitivity to ATP modulation are thought to be mediated by differential effects of ATP binding to specific motifs present in the receptors. Three glycine-rich regions (G*X*G*XX*G), reminiscent of Walker A motifs found in many ATPases and GTPases, are present in the $InsP_3R$ sequences (18, 19). One such motif, termed the ATPA site, is unique to $InsP_3R1$ and is presumed to account for the higher sensitivity of this isoform to modulation by ATP (12, 20). The ATPB site is conserved among all three isoforms and is thought to account for the lower sensitivity of $InsP_3R3$ to ATP modulation, since it has a lower affinity for ATP than the ATPA site (12, 15). Although binding of ATP to these motifs has been observed, the effect of mutating these sites has not been thoroughly examined. $InsP_3R1$ harboring the

* This work was supported, in whole or in part, by National Institutes of Health Grants RO1-DK054568 and RO1-DE016999 (to D. I. Y.). The costs of publication of this article were defrayed in part by the payment of page charges. This article must therefore be hereby marked "*advertisement*" in accordance with 18 U.S.C. Section 1734 solely to indicate this fact.

[1] Supported by NIDCR, National Institutes of Health, Training Grant T32-DE07202.

[2] To whom correspondence should be addressed: 601 Elmwood Ave., Box 711, Rochester, NY 14625. Tel.: 585-273-2154; Fax: 585-273-2652; E-mail: David_Yule@urmc.rochester.edu.

[3] The abbreviations used are: $InsP_3$, inositol 1,4,5-trisphosphate; $InsP_3R$, $InsP_3$ receptor(s); GST, glutathione *S*-transferase; TNP-ATP, trinitrophenyl-ATP; ICM, intracellular medium; NP_o, channel open probability.

Opisthotonos mutation disrupts the ATPA site, and this construct exhibited a reduced sensitivity to ATP modulation when compared with wild type in lipid bilayers (20). However, no effect was observed on Ca^{2+} signaling in DT40-3KO cells expressing this mutant receptor (20). An additional site, termed ATPC, is only found in the $S2^-$ $InsP_3R1$ splice variant. Prior work from our laboratory established that a mutation in the ATPC site prevented phosphorylation of the receptor by PKA (21). To date, no studies exist to support the idea that the ATPB sites mediate any functional effects of ATP binding to $InsP_3R$.

The goal of this study was to define what role the ATPB sites has in determining the sensitivity of $InsP_3R2$ and $InsP_3R3$ to ATP modulation. In order to address this question, individual wild type or mutant isoforms were stably expressed in DT40-3KO cells, which are null for $InsP_3R$ (22). ATP modulation of $InsP_3R$ was examined in permeabilized cells using endoplasmic reticulum luminal Ca^{2+} measurements and using whole cell single channel measurements (25, 26). Our findings establish that, contrary to prior reports, $InsP_3R2$ is enhanced by ATP and is actually more sensitive to ATP modulation than $InsP_3R3$. Further, we demonstrate that despite the two receptors harboring identical ATP binding sites, the effects of mutating these sites were dramatically different. Ablation of the ATPB site in $InsP_3R2$ completely abolished any modulatory effects of ATP, whereas a similar mutation in $InsP_3R3$ had no effect on the ability of ATP to enhance receptor activity. Finally, we show that ATP binding to the ATPB site in $InsP_3R2$ exerts control of the frequency and amplitude of Ca^{2+} signals in cells expressing $InsP_3R2$.

EXPERIMENTAL PROCEDURES

Construction of GST Fusion Proteins—GST fusion proteins were created using the pFN2A (GST) Flexi Vector (Promega, Madison, WI). Nucleotides corresponding to amino acids 1943–2013 of mouse $InsP_3R2$ and amino acids 1849–1944 of rat $InsP_3R3$ were amplified by PCR. SgfI and PmeI restriction sites were incorporated into the DNA primers used for PCR amplification. The PCR products were ligated into pFN2A at the SgfI and PmeI sites. This creates a fusion construct with GST at the NH_2 terminus of the $InsP_3R$ sequences and a tobacco etch virus protease recognition sequence in between to allow cleavage and removal of GST. Constructs with mutations corresponding to G1971A in $InsP_3R2$ and G1922A in $InsP_3R3$ were created and were verified by sequencing. Expression constructs were used to transform BL21 (DE3) pLysS cells (Promega, Madison, WI) for protein production. Production of recombinant protein, removal of the GST tag, and subsequent purification of $InsP_3R$ protein was accomplished as previously described (21).

ATP Binding Assay—The fluorescent ATP analog trinitrophenyl-ATP (TNP-ATP) (Invitrogen), which increases fluorescence upon binding to protein (excitation, 403 nm; emission, 546 nm), was used to measure ATP binding to the purified $InsP_3R2$ and $InsP_3R3$ ATPB proteins as previously described (21). Increasing concentrations of TNP-ATP were added to 1 mg of purified protein, and fluorescence was measured using a PerkinElmer LS-5B luminescence spectrometer (Wellesley, MA).

Mutagenesis—Expression constructs harboring cDNA for mouse $InsP_3R2$ (6) and rat $InsP_3R3$ (23) were used as templates for mutagenesis. A two-step QuikChange (Stratagene, La Jolla, CA) mutagenesis strategy (24) was used to introduce G5940C, G5946C, and G5955C point mutations into the $InsP_3R2$ cDNA. These mutations code for amino acid substitutions: G1969A, G1971A, and G1974A, respectively. Sequencing of the entire $InsP_3R2$ coding region (GeneWiz, South Plainfield, NJ) confirmed the correct incorporation of the desired mutations but also revealed an additional spurious deviation from the published sequence (T1044A, leading to amino acid substitution I337N). This substitution is unlikely to result in grossly altered receptor function, since the Ca^{2+} release rates achieved were comparable between the wild type and ΔATPB receptors in the absence of ATP over a range of $[InsP_3]$ (see Figs. 2 and 5). Splice-overlap extension PCR of an internal 4225-base pair KpnI fragment of $InsP_3R3$ was used to introduce G5893C, G5899C, and G5908C. These mutations code for amino acid substitutions: G1920A, G1922A, and G1925A, respectively. Correct incorporation of the mutants and the integrity of the amplified region were verified by DNA sequencing (GeneWiz, South Plainfield, NJ).

Creation of Stable $InsP_3R2$ and $InsP_3R3$-expressing DT40-3KO Cell Lines—Wild type and mutated $InsP_3R2$ and $InsP_3R3$ constructs were linearized with MfeI and NruI, respectively. Linearized constructs were introduced into DT40-3KO cells by nucleofection using solution T and program B23 as per the manufacturer's instructions (Amaxa, Cologne, Germany). After nucleofection, the cells were incubated in growth medium for 24 h prior to dilution in selection medium containing 2 mg/ml Geneticin (Invitrogen). Cells were then seeded into 96-well tissue culture plates at ~1000 cells/well and incubated in selection medium for at least 7 days. Wells exhibiting growth after the selection period were picked for expansion.

Permeabilized Cell Ca^{2+} Measurements—$InsP_3R2$- and $InsP_3R3$-expressing stable DT40-3KO cells were loaded with 20 μM furaptra-AM (Teflabs, Austin, TX) at 39 °C for 30 min in a HEPES-buffered physiological saline solution (HEPES-PSS) containing 5.5 mM glucose, 137 mM NaCl, 0.56 mM $MgCl_2$, 4.7 mM KCl, 1 mM Na_2HPO_4, 10 mM HEPES (pH 7.4), 1.2 mM $CaCl_2$, and 1% (w/v) bovine serum albumin. Furaptra-loaded cells were permeabilized by superfusion for 1–2 min with 40 μM β-escin in intracellular medium (ICM) containing 125 mM KCl, 19 mM NaCl, 10 mM HEPES, 1 mM EGTA (pH 7.3). Permeabilized cells were then washed in ICM without β-escin for 15 min to facilitate removal of cytosolic dye, and the cells were then superfused in ICM containing 1.4 mM $MgCl_2$, 3 mM Na_2ATP, and 0.650 mM $CaCl_2$ (free $[Ca^{2+}]$ of 200 nM, calculated using MAXCHELATOR) to load the intracellular stores. The free $[Ca^{2+}]$ was subsequently maintained at a constant 200 nM throughout all experimental maneuvers and was verified by fluorescent measurement of free Ca^{2+} in solutions. Prior to application of $InsP_3$, the cells were superfused in ICM without $MgCl_2$ for 1 min to disable SERCA activity. The unidirectional flux of Ca^{2+} upon $InsP_3$ application was then monitored in the same solution containing various concentrations of $InsP_3$ and ATP by monitoring the emission of the dye above 505 nm following excitation at 340 and 380 nm (exposure for 20 ms, once per second), using a TILL Photonics imaging system. Following the removal of $InsP_3$, refilling of the stores to allow repeated stimulations was accomplished by superfusion of ICM contain-

ing $MgCl_2$ and ATP. Ca^{2+} release events were averages of the 30–50 cells in a field of view. Rates of Ca^{2+} release were estimated from these average responses by fitting the initial 30-s period of decreasing fluorescence to a single exponential function (GraphPad Prism, San Diego, CA).

Single $InsP_3R2$ Channel Measurements—Whole cell patch clamp recordings of single $InsP_3R2$ channel activity (25, 26) were taken from DT40-3KO cells stably expressing mouse $InsP_3R2$. K^+ was utilized as the charge carrier in all experiments, and free Ca^{2+} was clamped at 200 nM to favor activation of $InsP_3R$ (bath: 140 mM KCl, 10 mM HEPES, 500 μM BAPTA, 250 nM free Ca^{2+} (pH 7.1); pipette: 140 mM KCl, 10 mM HEPES, 100 μM BAPTA, 200 nM free Ca^{2+}, 5 mM Na_2-ATP unless otherwise noted (pH 7.1)). Borosilicate glass pipettes were pulled and fire polished to resistances of about 20 megaohms. Following establishment of stable high resistance seals, the membrane patches were ruptured to form the whole-cell configuration with resistances of >5 gigaohms and capacitances of >8 picofarads. Currents were recorded under voltage clamp conditions at the indicated potentials using an Axopatch 200B amplifier and pClamp 9. Channel recordings were digitized at 20 kHz and filtered at 5 kHz with a −3 decibel, 4-pole Bessel filter. Activity was typically evident essentially immediately following breakthrough with $InsP_3$ in the pipette. Analyses were performed using the event detection protocol in Clampfit 9. Channel openings were detected by half-threshold crossing criteria. We assumed that the number of channels in any particular cell is represented by the maximum number of discrete stacked events observed during the experiment. The P_o was calculated using the multimodal distribution for the open and closed current levels.

Digital Imaging of $[Ca^{2+}]_i$ in Intact Cells—$InsP_3R2$- and $InsP_3R3$-expressing stable DT40-3KO cells were washed once in a HEPES-PSS containing 1% (w/v) bovine serum albumin. Cells were then resuspended in bovine serum albumin HEPES-PSS with 1 μM Fura-2/AM (Teflabs Inc., Austin, TX), placed on a 15-mm glass coverslip in a low volume perfusion chamber, and allowed to adhere for 20 min at room temperature. Cells were perfused continuously for 10 min with HEPES-PSS before experimentation to allow complete Fura-2 deesterification. $[Ca^{2+}]_i$ imaging was performed using an inverted epifluorescence Nikon microscope with a ×40 oil immersion objective lens (numerical aperture, 1.3). Cells were excited alternately with light at 340 and 380 nm (± 10-nm bandpass filters, Chroma, Rockingham, VT) using a monochrometer (TILL Photonics, Pleasanton, CA). Fluorescence images were captured and digitized with a digital camera driven by TILL Photonics software. Images were captured every 2 s with an exposure of 20 ms and 4 × 4 binning. 340/380 ratio images were calculated online and stored immediately to a hard disk. Intracellular Ca^{2+} transients were analyzed for frequency and amplitude using the template detection option from the event detection protocol in pClamp9. Transients with a change in 340/380 less than 0.05 ratio units were discarded.

Microsomal Preparation and Western Blotting—Microsomal membranes were prepared from nontransfected DT40-3KO or DT40-3KO cells stably expressing $InsP_3R$ essentially as previously described (27). Briefly, cells were pelleted and resuspended in homogenization buffer (5 mM NaN_3, 0.1 mM EGTA, 1 mM β-mercaptoethanol, 20 mM HEPES, pH 7.4). After homogenization by 60 strokes of a motor-driven Teflon homogenizer, samples were spun in a tabletop centrifuge at 2000 rpm for 10 min. Supernatants were spun at 100,000 × *g* (50,000 rpm in Beckman centrifuge with a TLA100.3 rotor). Membrane pellets were solubilized in Laemmli running buffer, and protein concentrations were determined using Amido Black. Equal amounts of membrane proteins were separated on 5% polyacrylamide gels and transferred to nitrocellulose. Membranes were probed with antibodies specific for $InsP_3R2$ or $InsP_3R3$. The $InsP_3R2$ antibody was directed against a unique sequence from rat $InsP_3R2$ (^{320}PDYRDAQNEGKTVRDGELP^{338}). The antibody was produced by Pocono Rabbit Farms and Laboratories (Canadensis, PA). The $InsP_3R3$ antibody was from BD Biosciences.

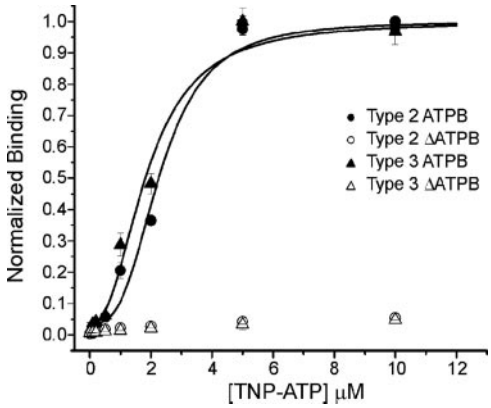

FIGURE 1. **TNP-ATP binds to ATPB sites.** ATP binding to the ATPB sites from $InsP_3R2$ and $InsP_3R3$ were assessed by monitoring the fluorescence of TNP-ATP as described under "Experimental Procedures." TNP-ATP binds to purified ATPB from $InsP_3R2$ with an EC_{50} of 2.3 ± 0.2 μM (*filled circles*) and binds to purified ATPB from $InsP_3R3$ with an EC_{50} of 1.9 ± 0.2 μM (*filled triangles*). TNP-ATP does not bind to mutated ATPB sites from $InsP_3R2$ (*open circles*) and $InsP_3R3$ (*open triangles*).

RESULTS

The ATPB Site from $InsP_3R2$ Binds TNP-ATP—ATP has been shown to bind to full-length $InsP_3R1$ and $InsP_3R3$ as well as to purified peptides containing the ATPB sites from both receptor isoforms; however, the ability of ATP to bind to the ATPB site in $InsP_3R2$ has not been tested (12, 28). This is an important consideration, since a possible explanation for the lack of functional effects of ATP on $InsP_3R2$ is that the ATPB site from $InsP_3R2$ cannot bind ATP. In order to compare the ATP binding properties of the ATPB sites from $InsP_3R2$ and $InsP_3R3$, we generated cDNA constructs encoding GST fused to residues 1943–2013 of $InsP_3R2$ and to residues 1849–1944 of $InsP_3R3$. These fusion proteins contain the glycine-rich putative ATPB sites as well as enough flanking sequence to allow for efficient protein expression and purification.

After elution from the GST-agarose and proteolytic removal of the GST tag, binding to the purified ATPB sites was assessed using a TNP-ATP binding assay. Increasing amounts of TNP-ATP were added to 1-mg samples of the purified ATPB proteins, and greater fluorescence indicated binding of the TNP-ATP to the purified proteins. As shown in Fig. 1, TNP-ATP can

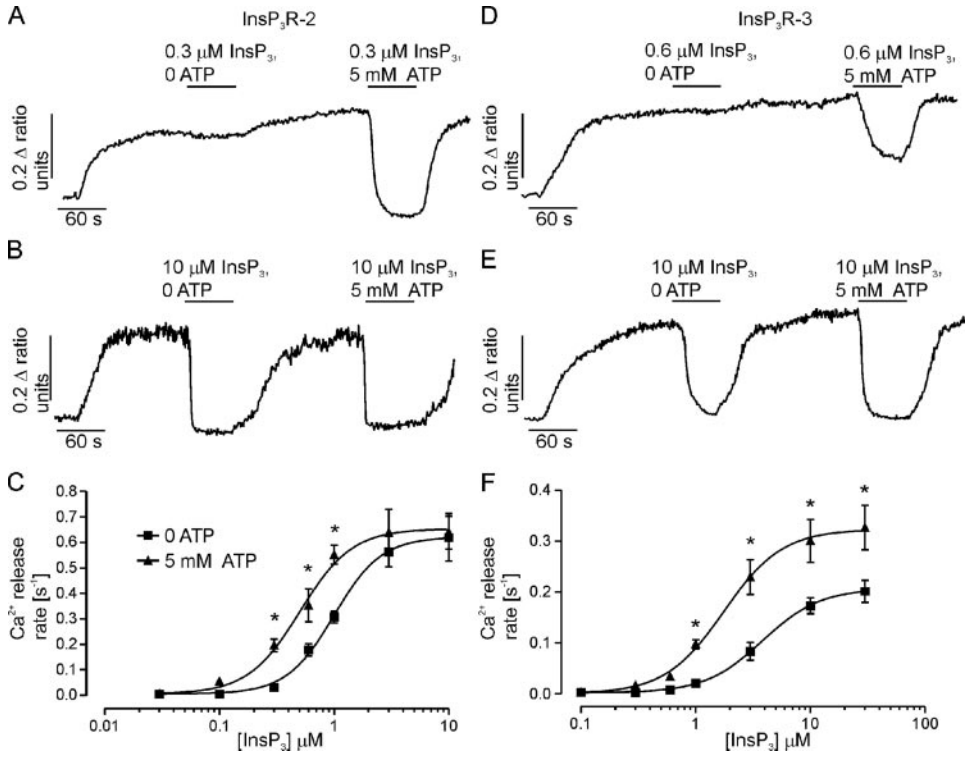

FIGURE 2. **The effects of ATP on $InsP_3$-induced Ca^{2+} release from $InsP_3R2$ and $InsP_3R3$.** Endoplasmic reticulum luminal Ca^{2+} measurements were obtained from cells stably expressing mouse $InsP_3R2$ (*A* and *B*) or rat $InsP_3R3$ (*D* and *E*). Cells were loaded with furaptra and permeabilized with β-escin as described under "Experimental Procedures." 5 mM ATP increased the $InsP_3$-induced Ca^{2+} release from $InsP_3R2$ when low [$InsP_3$] was used (*A*) but not when high [$InsP_3$] was used (*B*). *D* and *E*, results obtained from similar experiments using cells expressing rat $InsP_3R3$. ATP enhances $InsP_3$-induced Ca^{2+} release from $InsP_3R3$ when using low (*D*) or high (*E*) [$InsP_3$]. *C* and *F*, concentration-response relationships for $InsP_3$ from cells expressing $InsP_3R2$ (*C*) or $InsP_3R3$ (*F*) in the absence or presence of 5 mM ATP. Each point is the mean ± S.E. from at least four experiments. Ca^{2+} release rates were calculated by fitting the average time course from the first 30 s of $InsP_3$ application from 30–50 cells to a single exponential. *, $p \leq 0.05$; Student's unpaired *t* test.

readily bind to the ATPB sites from both $InsP_3R2$ and $InsP_3R3$, as indicated by the increase in fluorescence with increasing concentrations of TNP-ATP. Additionally, the EC_{50} values for TNP-ATP binding were similar for both proteins, indicating similar affinities of TNP-ATP for the two binding sites. This could be expected given the high degree of similarity between the receptors in this region but does not necessarily mean that the affinities are the same in the context of the whole receptor. Determination of the absolute affinity of either isoform for ATP was not tenable by this method, because binding was not determined in the context of the full-length receptor and because TNP-ATP binds to proteins with a higher affinity than does unlabeled ATP (29). Even with these caveats, the results clearly show that the ATPB site from $InsP_3R2$ can bind ATP.

ATP Enhances the Activities of $InsP_3R2$ and $InsP_3R3$—Given that the ATPB from $InsP_3R2$ binds ATP, it is somewhat surprising that functional effects of ATP have not been observed for this isoform. It should be noted that previous studies examining the effects of ATP on $InsP_3R2$ used saturating $InsP_3$ concentrations, raising the possibility that any effects of ATP on $InsP_3R2$ were masked as a result of maximal stimulation (13, 15). In order to examine the effects of ATP on $InsP_3R$ function over the full range of $InsP_3$ concentrations, we generated DT40-3KO cell lines stably expressing either mammalian $InsP_3R2$ or $InsP_3R3$ in isolation.

Cells expressing $InsP_3R2$ or $InsP_3R3$ were loaded with the low affinity Ca^{2+} sensing dye furaptra, and unidirectional luminal Ca^{2+} measurements were made in β-escin permeabilized cells. $InsP_3R$ activity was determined by fitting the release events to single exponentials. Ca^{2+} release rates were measured over a range of $InsP_3$ concentrations in the presence and absence of 5 mM ATP in order to observe the effects of ATP on $InsP_3R$ function under varied levels of stimulation. Interestingly, the ability of ATP to enhance Ca^{2+} release from $InsP_3R2$ was strictly dependent on the concentration of $InsP_3$ used for stimulation. Representative recordings from $InsP_3R2$-expressing cells treated with low (0.3 μM) or high (10 μM) $InsP_3$ in the presence and absence of 5 mM ATP are shown in Fig. 2, *A* and *B*, respectively. ATP clearly enhances Ca^{2+} release in response to $InsP_3$ levels below 3 μM but is without effect if [$InsP_3$] is higher (Fig. 2*C*). 5 mM ATP caused a 2-fold shift in the EC_{50} for $InsP_3$ in cells expressing $InsP_3R2$ (Fig. 2*C*). In contrast, 5 mM ATP enhanced the Ca^{2+} release rate from cells expressing $InsP_3R3$ at all $InsP_3$ concentrations tested (Fig. 2, *D–F*). These data establish for the first time that, in a fashion similar to $InsP_3R1$ and $InsP_3R3$, ATP positively modulates $InsP_3R2$. Additionally, the results highlight possible important differences in the behavior of the receptors under maximal levels of stimulation. Specifically, $InsP_3R3$ activity is enhanced by ATP at supermaximal $InsP_3$ concentrations, whereas $InsP_3R2$ is only subject to modulation at submaximal [$InsP_3$].

Further evidence to support the premise that ATP can modulate $InsP_3R2$ was gained by measuring single $InsP_3R2$ channel activity in DT40 cells. Taylor and co-workers (25, 26) and Schug *et al.* (30) recently reported that small numbers of $InsP_3R$ are present in the plasma membranes of DT40 cells, which allows recording of single $InsP_3R$ in whole cell mode of the patch clamp technique (25, 26, 30). We first confirmed that $InsP_3R2$ is also present in the plasma membrane of DT40 cells stably expressing the receptor. $InsP_3R2$ channel activity was dependent on $InsP_3$, since no activity was observed in cells without $InsP_3$ in the pipette ($n = 5$ cells, >50 min of total recording time; data not shown). During these experiments, ATP (5 mM) was in the pipette, indicating that ATP is unable to stimulate channel openings in the absence of $InsP_3$. Furthermore, channel activity was absent in nontransfected cells, and heparin blocked the activity in transfected cells with 10 μM $InsP_3$ in the pipette ($n = 5$ cells; >50 min of total recording time; data not

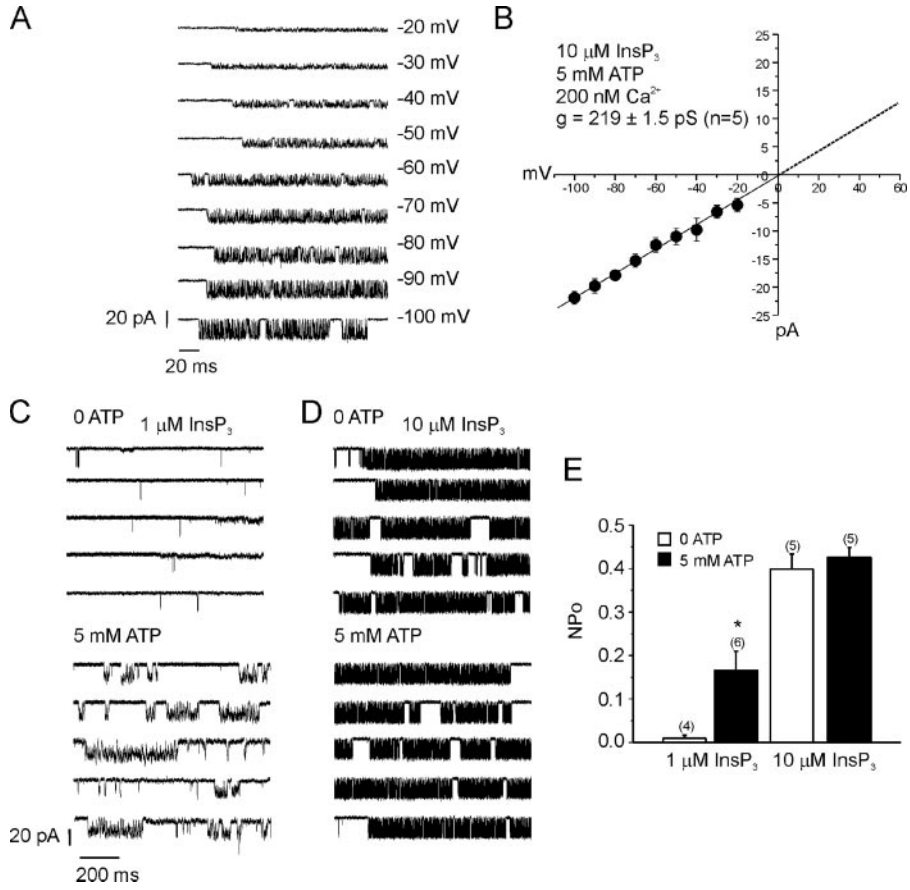

FIGURE 3. **ATP increases the single channel open probability $InsP_3R2$ at low [$InsP_3$].** Single channel activity of plasma membrane-resident $InsP_3R2$ was measured in whole cell patch clamp mode. *A*, representative recordings from a cell expressing $InsP_3R2$ and held at the indicated voltages with 10 μM $InsP_3$ in the pipette. *B*, current-voltage relationship indicating a slope conductance for K^+ of 219 ± 1.9 picosiemens. *C*, 5 mM ATP increased the NP_o of $InsP_3R2$ when low (1 μM) $InsP_3$ was included in the pipette (0.01 ± 0.007 with 0 ATP *versus* 0.16 ± 0.04 with 5 mM ATP. Recordings are from different cells held at −100 mV with 1 μM $InsP_3$ and the indicated [ATP]. *D*, no effects of 5 mM ATP were observed in recordings from cells in which 10 μM $InsP_3$ was used (0.40 ± 0.03 *versus* 0.42 ± 0.02). Recordings are from different cells held at −100 mV with 10 μM $InsP_3$ and the indicated [ATP]. *E*, the mean NP_o ± S.E. and number of cells for each condition. *, $p \leq 0.05$; Student's unpaired *t* test.

shown). Fig. 3*A* shows representative recordings from a cell held at various membrane potentials with 10 μM $InsP_3$ in the pipette, and Fig. 3*B* shows the average single channel current-voltage relationship from five such cells.

We next tested for effects of ATP on the open probability of $InsP_3R2$ using low (1 μM) or high (10 μM) $InsP_3$ to stimulate channel activity. Consistent with results obtained in luminal Ca^{2+} measurements (Fig. 2); the effects of ATP were dependent on the concentration of $InsP_3$ used for activation. As shown in Fig. 3*C*, in the presence of 1 μM $InsP_3$, the NP_o of $InsP_3R2$ was 10-fold greater when 5 mM ATP was included in the pipette compared with the absence of ATP. The activity of $InsP_3R2$, however, was not enhanced by 5 mM ATP when 10 μM $InsP_3$ was included in the pipette (0.40 ± 0.03 *versus* 0.42 ± 0.02) (Fig. 3*D*).

Different Sensitivities of $InsP_3R2$ and $InsP_3R3$ to ATP Modulation—The experiments outlined above tested the effects of presumably saturating [ATP] on $InsP_3R$ activity. However, these maneuvers did not address whether $InsP_3R2$ and $InsP_3R3$ have similar ATP sensitivities. Therefore, we next sought to compare the sensitivities of $InsP_3R2$ and $InsP_3R3$ to ATP modulation under similar experimental settings. ATP levels were varied between 0 and 5 mM at fixed $InsP_3$ and Ca^{2+} concentrations. 0.3 μM $InsP_3$ was chosen for $InsP_3R2$-expressing cells, and 1.0 μM $InsP_3$ was used for $InsP_3R3$-expressing cells, because these $InsP_3$ concentrations elicited similar Ca^{2+} release rates from both receptor populations in the absence of ATP (0.024 ± 0.007 s^{-1} for $InsP_3R2$ and 0.019 ± 0.004 s^{-1} for $InsP_3R3$). In addition, the -fold increases in Ca^{2+} release rates with 5 mM ATP were similar (~9-fold for $InsP_3R2$ and ~8-fold for $InsP_3R3$). Fig. 4 shows the results of representative Ca^{2+} release experiments using various levels of ATP for cells expressing $InsP_3R2$ (Fig. 4*A*) or $InsP_3R3$ (Fig. 4*B*). Cells expressing $InsP_3R2$ exhibited a dramatically higher sensitivity to ATP under these conditions, with an EC_{50} for ATP of ~41 μM *versus* ~400 μM for cells expressing $InsP_3R3$ (Fig. 4*C*).

The Consequences of Mutated ATPB Sites on the Modulatory Effects of ATP on $InsP_3R$—The above experiments highlight important differences in the Ca^{2+} release behavior of the two isoforms, which is especially interesting given that the receptors each contain a single identical putative ATP binding domain. Experiments were performed to determine if these ATPB sites are, in fact, responsible for the observed functional effects of ATP on both receptors. We generated stable DT40 cell lines expressing ATPB-deficient $InsP_3R2$ and $InsP_3R3$. Initially, stable cell lines were generated with receptors harboring single glycine-alanine substitutions (G1971A for $InsP_3R2$ and G1922A for $InsP_3R3$). Cells expressing each of these mutant receptors still exhibited positive modulation by ATP in Ca^{2+} release experiments (data not shown). This was surprising, since analogous mutations abolished TNP-ATP binding (Fig. 1), but may reflect different binding determinants for the full-length receptor. Additionally, ATP may bind to the ATPB site in a manner different from that of the bulkier TNP-ATP. In order to ensure that ATP could not interact with the ATPB sites, more severe mutations were generated by substituting glycines 1969, 1971, and 1974 in $InsP_3R2$ and glycines 1920, 1922, and 1925 in $InsP_3R3$ with alanines. The effect of ATP on $InsP_3$-induced Ca^{2+} release was then examined in permeabilized cells expressing these mutant receptors. In contrast to cells expressing wild type receptor, in cells expressing mutated $InsP_3R2$, 5 mM ATP had no effect on the Ca^{2+} release rates at all $InsP_3$ levels tested (Fig. 5). These data establish the

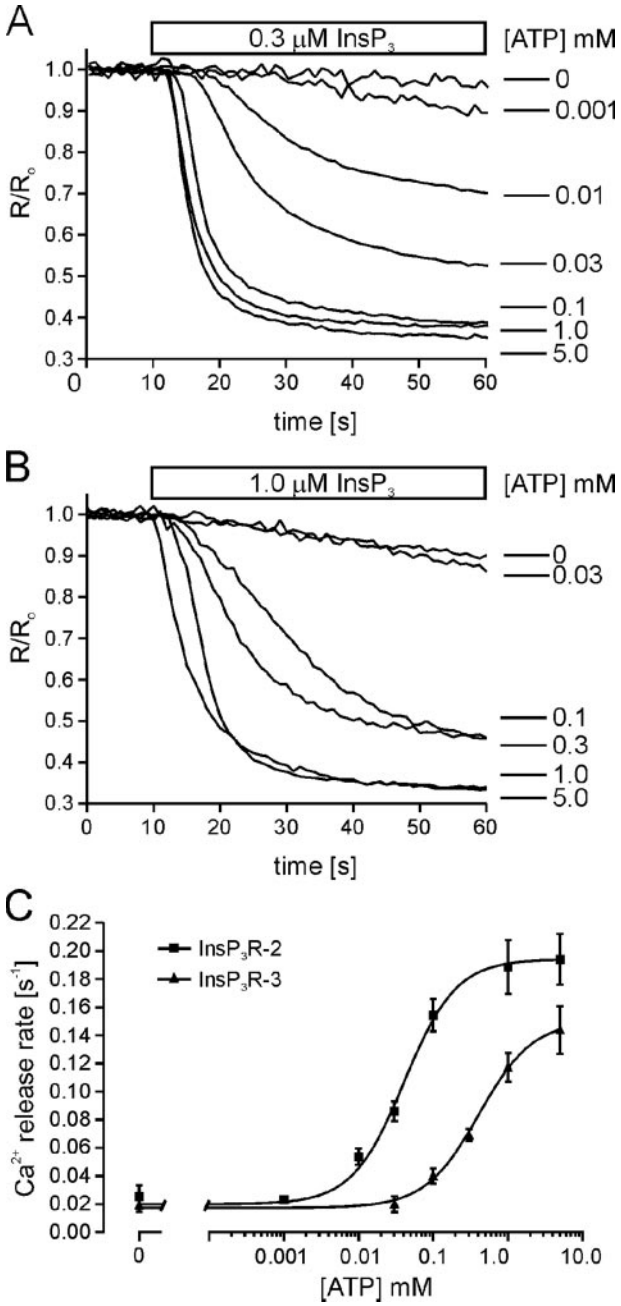

FIGURE 4. **$InsP_3R2$ is more sensitive than $InsP_3R3$ to ATP modulation.** Cells stably expressing $InsP_3R2$ or $InsP_3R3$ were loaded with furaptra and permeabilized as described under "Experimental Procedures." *A*, representative Ca^{2+} release events from cells stably expressing $InsP_3R2$. 0.3 μM $InsP_3$ was applied along with the indicated [ATP]. *B*, representative Ca^{2+} release events from cells stably expressing $InsP_3R3$ and stimulated with 1.0 μM $InsP_3$ along with the indicated [ATP]. Each trace is the average from 30–50 cells and was normalized to the average 340/380 ratio from the 10 frames prior to $InsP_3$ application. *C*, concentration-response relationships for ATP. Cells expressing $InsP_3R2$ exhibit an EC_{50} for ATP of 41 μM, and cells expressing $InsP_3R3$ exhibit an EC_{50} for ATP of 400 μM. Each point is the mean ± S.E. from at least four experiments. Ca^{2+} release rates were determined by fitting the average time course from the first 30 s of $InsP_3$ application from 30–50 cells to a single exponential.

ATPB site as the only functionally relevant ATP binding site in $InsP_3R2$. The results obtained from a mutated $InsP_3R3$ were, however, dramatically different. In contrast to $InsP_3R2$, the effects of ATP were retained in cells expressing an ATPB-deficient $InsP_3R3$ (Fig. 6). In a manner similar to the wild type receptor, the enhanc-

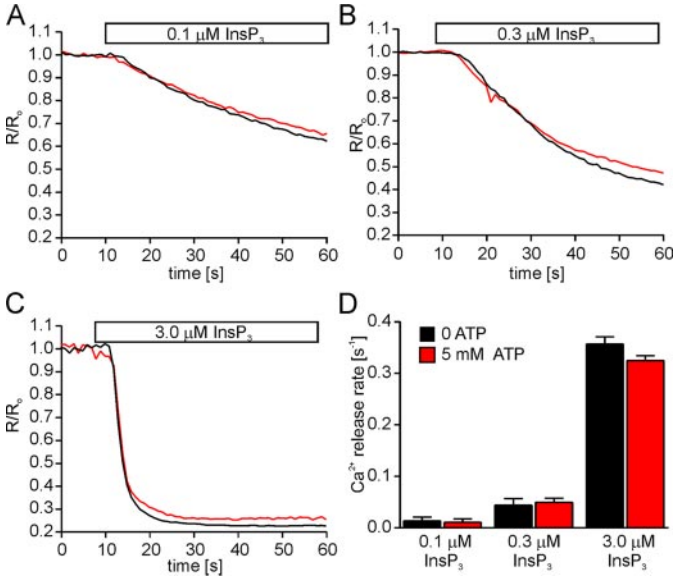

FIGURE 5. **The ATPB site is required for ATP modulation of $InsP_3R2$.** The ATPB site was mutated in $InsP_3R2$ by substituting glycines 1969, 1971, and 1974 with alanines. Cells stably expressing mutated $InsP_3R2$ ($InsP_3R2$-ΔATPB) were loaded with furaptra and permeabilized as described under "Experimental Procedures." *A–C*, representative Ca^{2+} release events from cells stimulated with the indicated [$InsP_3$] in the absence (*black*) or presence (*red*) of 5 mM ATP. Each *trace* is the average from 30–50 cells and was normalized to the average 340/380 ratio from the 10 frames prior to $InsP_3$ application. *D*, the mean Ca^{2+} release rates ± S.E. from these experiments ($n = 3$ at 0.1 μM $InsP_3$: 0.01 ± 0.007 s^{-1} at zero ATP and 0.01 ± 0.006 s^{-1} at 5 mM ATP; $n = 4$ at 0.3 μM $InsP_3$: 0.05 ± 0.009 s^{-1} at zero ATP and 0.05 ± 0.006 s^{-1} at 5 mM ATP; $n = 3$ at 3.0 μM $InsP_3$: 0.36 ± 0.013 s^{-1} at zero ATP and 0.32 ± 0.009 s^{-1} at 5 mM ATP).

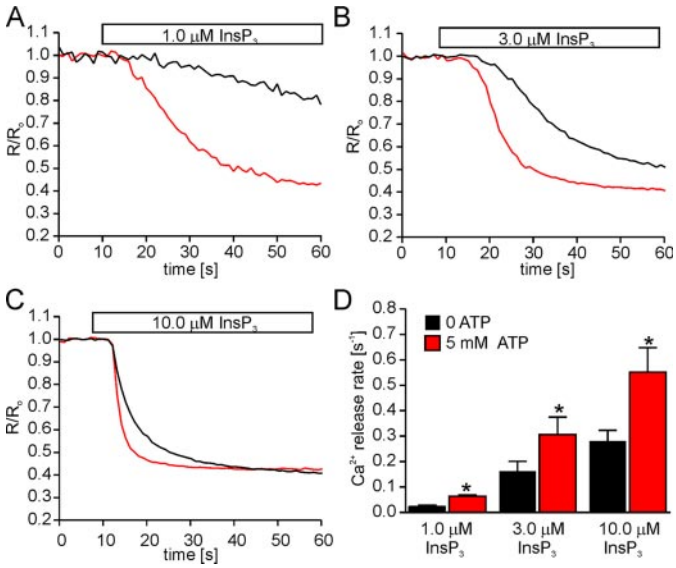

FIGURE 6. **The ATPB site is not required for ATP modulation of $InsP_3R3$.** The ATPB site is required for ATP modulation of $InsP_3R3$. The ATPB site was mutated in $InsP_3R3$ by substituting glycines 1920, 1922, and 1925 with alanines. Cells stably expressing mutated $InsP_3R3$ ($InsP_3R3$-ΔATPB) were loaded with furaptra and permeabilized as described under "Experimental Procedures." *A–C*, representative Ca^{2+} release events from cells stimulated with the indicated [$InsP_3$] in the absence (*black*) or presence (*red*) of 5 mM ATP. Each trace is the average from 30–50 cells and is normalized to the average 340/380 ratio from the 10 frames prior to $InsP_3$ application. *D*, the mean Ca^{2+} release rates ± S.E. from these experiments ($n = 4$ at 1.0 μM $InsP_3$: 0.02 ± 0.006 s^{-1} at zero ATP and 0.06 ± 0.005 s^{-1} at 5 mM ATP; $n = 6$ at 3.0 μM $InsP_3$: 0.16 ± 0.04 s^{-1} at zero ATP and 0.31 ± 0.007 s^{-1} at 5 mM ATP; $n = 6$ at 10.0 μM $InsP_3$ 0.28 ± 0.04 s^{-1} at zero ATP and 0.55 ± 0.09 s^{-1} at 5 mM ATP). *, $p \leq .05$; Student's paired *t* test.

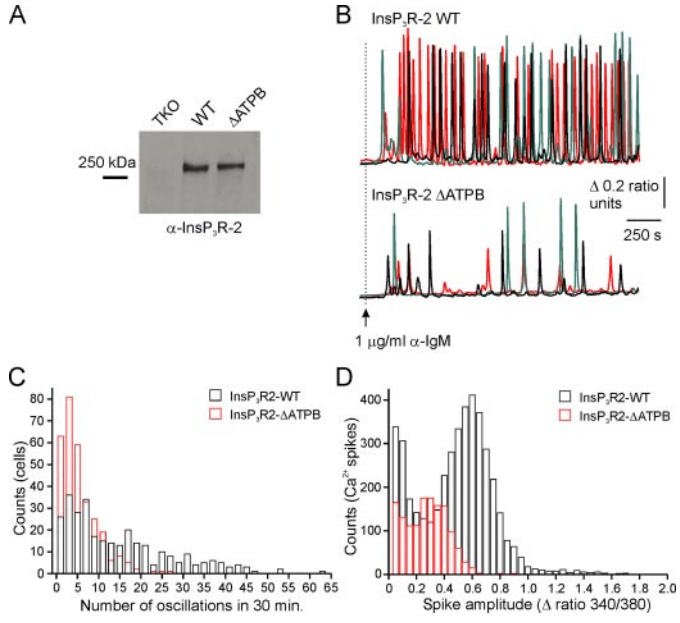

FIGURE 7. **Mutating the ATPB site in $InsP_3R2$ affects BCR-induced Ca^{2+} signaling.** *A*, microsomal membranes were prepared from nontransfected DT40-3KO cells (*TKO*) and from cells stably expressing either wild type $InsP_3R2$ (*$InsP_3R2$*) or $InsP_3R2$-ΔATPB (*ΔATPB*). 50 μg of membrane protein were separated by SDS-PAGE, transferred to nitrocellulose, and probed with an antibody directed against $InsP_3R2$. *B*, representative Fura-2 recordings from three individual cells (*black traces*, *red traces*, and *green traces*) expressing either $InsP_3R2$ (*top*) or $InsP_3R2$-ΔATPB (*bottom*) and stimulated with 1 μg/ml anti-IgM where indicated by the *arrow*. *C*, a histogram of the number of oscillations/cell over 30 min of stimulation (*black outlines*, $InsP_3R2$; *red outlines*, $InsP_3R2$-ΔATPB). *D*, a histogram of the amplitudes of the Ca^{2+} spikes counted in *C*. *WT*, wild type.

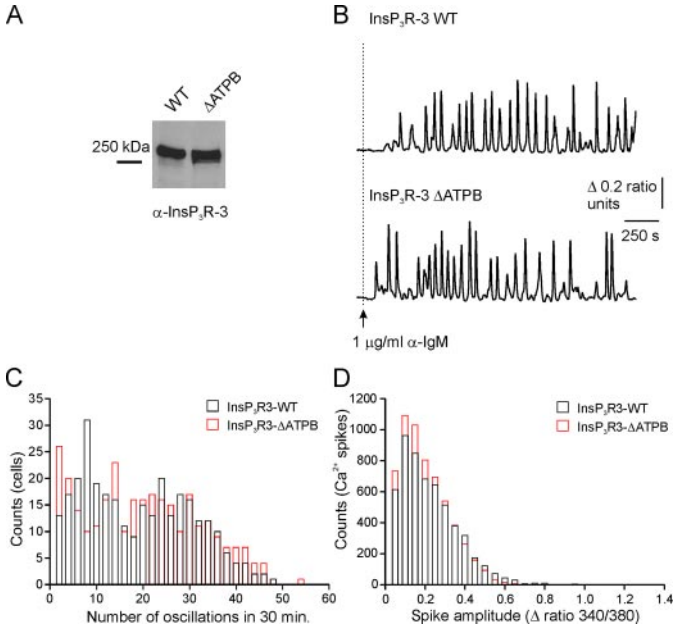

FIGURE 8. **Mutating the ATPB site in $InsP_3R3$ does not affect BCR-induced Ca^{2+} signaling.** *A*, microsomal membranes were prepared from cells stably expressing wild type $InsP_3R3$ (*$InsP_3R3$*) or $InsP_3R3$-ΔATPB (*ΔATPB*). 50 μg of membrane protein were separated by SDS-PAGE, transferred to nitrocellulose, and probed with an antibody directed against $InsP_3R3$. *B*, representative Fura-2 recordings from individual cells expressing either $InsP_3R3$ (*top*) or $InsP_3R3$-ΔATPB (*bottom*) and stimulated with 1 μg/ml anti-IgM where indicated by the *arrow*. *C*, a histogram of the number of oscillations per cell over 30 min of stimulation (*black outlines*, $InsP_3R3$; *red outlines*, $InsP_3R3$-ΔATPB). *D*, a histogram of the amplitudes of the Ca^{2+} spikes counted in *C*. *WT*, wild type.

ing effects of ATP were observed at all tested [$InsP_3$].

The Effects of ATPB-deficient $InsP_3R$ on the Intracellular Ca^{2+} Signals—DT40 cells generate repetitive intracellular Ca^{2+} spikes when stimulated with an antibody directed against IgM (13, 31). Ca^{2+} signals are initiated by cross-linking of the B-cell receptor and are phospholipase C-γ2- and $InsP_3R$-dependent (13, 22, 32). We took advantage of this endogenous signaling pathway to examine the effects of $InsP_3R$ mutations on the intracellular Ca^{2+} responses of cells stably expressing wild type and ΔATPB mammalian $InsP_3R$. Consistent with the reported results from DT40 cells expressing chicken $InsP_3R2$ in isolation, cells expressing mouse $InsP_3R2$ exhibited robust oscillatory intracellular Ca^{2+} responses after stimulation with 1 μg/ml anti-IgM (Fig. 7*B*, *top*). These signals typically initiated within 2–3 min of antibody application and persisted throughout the experimental time course of 30 min. Similar amounts of $InsP_3R2$ were detected in Western blots from cell lines expressing wild type and ATPD-mutated Ins_3R2 (Fig. 7*A*). The properties of the Ca^{2+} signals in cells expressing the mutated receptor, however, were dramatically different from the patterns elicited from cells expressing the wild type receptor. The properties of the signals were, however, dramatically different from the patterns elicited from cells expressing the wild type receptor (Fig. 7*B*, *bottom*). The mean observed number of oscillations was significantly reduced in $InsP_3R2$-ΔATPB-expressing cells compared with wild type $InsP_3R$-expressing cells (5.2 ± 0.9 *versus* 14.1 ± 1.4 spikes/cell over 30 min; $n = 6$; 300 cells; $p \leq 0.05$; Student's unpaired *t* test). Additionally, the mean amplitude of the spikes was also reduced in $InsP_3R2$-ΔATPB-expressing cells (0.26 ± 0.03 *versus* 0.49 ± 0.03 Δ ratio units; $n = 6$; 300 cells; $p \leq 0.05$; Student's unpaired *t* test).

Cells expressing rat $InsP_3R3$ also exhibited repetitive intracellular Ca^{2+} responses (Fig. 8*A*), suggesting that the mammalian isoform is able to support oscillatory responses in these cells. This contrasts with the observation that a similar stimulation of cells expressing endogenous chicken $InsP_3R3$ in isolation produced only monophasic Ca^{2+} responses (13), although anti-IgM-induced oscillations were also observed in another DT40-3KO cell line stably expressing rat $InsP_3R3$ (33). Consistent with the ATPB site having no effect on the enhancing effects of ATP in permeabilized cells (Fig. 6), the BCR-induced Ca^{2+} signals elicited from ATPB-mutated $InsP_3R3$-expressing cells were indistinguishable from signals elicited from wild type $InsP_3R3$-expressing cells (Fig. 8). The cell lines exhibited similar numbers of oscillations (17.9 ± 2.2 (wild type) *versus* 19.5 ± 2.0 (ΔATPB) spikes/cell over 30 min; $n = 5$; 300 cells) as well as similar mean spike amplitudes (0.21 ± 0.01 (wild type) *versus* 0.20 ± 0.02 (ΔATPB) Δ ratio units; $n = 5$; 300 cells).

DISCUSSION

The effects of ATP and related nucleotides on $InsP_3R1$ and $InsP_3R3$ function have been extensively studied in numerous systems, but ATP regulation of $InsP_3R2$ function has not been previously reported. Two prior studies have described $InsP_3R2$ as being insensitive to ATP modulation following activation with high [$InsP_3$] (13, 15). Further, the lack of ATP effects was shown to predominate in cells expressing $InsP_3R2$ in combina-

tion with the other isoforms (13). A major contribution of the present study is to demonstrate that ATP does, in fact, regulate $InsP_3R2$ but only at submaximal [$InsP_3$]. Additionally, $InsP_3R2$ exhibits a much higher sensitivity to ATP modulation than $InsP_3R3$ at these [$InsP_3$] values. Using a mutagenesis approach, we also demonstrate that, in contrast to $InsP_3R3$, this high sensitivity to ATP is mediated by the ATPB site present in $InsP_3R2$.

All of the effects of ATP observed in these experiments were determined in the absence of $MgCl_2$. Magnesium-bound ATP (MgATP) has been shown to modulate $InsP_3R1$ and $InsP_3R3$ in numerous studies (12, 14) but was not effective in nuclear patch clamp measurements of $InsP_3R1$ or $InsP_3R3$ (16, 17). We excluded $MgCl_2$ from experimental buffers for 1 min prior to and throughout stimulation with $InsP_3$ to prevent SERCA activation. Although allowing unidirectional measures of $InsP_3R$ function, this paradigm does not allow for an assessment of the effects of MgATP. We therefore cannot comment on whether MgATP, in particular, is able to modulate $InsP_3R2$ or $InsP_3R3$ function to the same extent as free ATP.

We also find that, in contrast to $InsP_3R2$, ATP increases both the efficacy and potency of $InsP_3$ in cells expressing $InsP_3R3$ in isolation. This divergence from cells expressing $InsP_3R2$ could be explained by an additional locus for ATP modulation in $InsP_3R3$ besides the Walker A-type ATPB site. The possibility of an additional site is likely, given that ablation of the ATPB site in $InsP_3R3$ did not eliminate the enhancing effects of ATP. Currently, no biochemical evidence for additional sites has been reported. $InsP_3R3$ was shown to cross-link with 8-azido-[α-^{32}P]ATP exclusively within a 95-kDa tryptic fragment that contains the ATPB site (28). It is formally possible that additional binding sites exist in the same fragment, but no sequence similarity to known ATP binding sequences, such as Walker motifs or cystathionine β-synthase-related domains (34), exists in this region or indeed any other region of $InsP_3R3$.

The lack of known additional ATP binding motifs in $InsP_3R3$ highlights the possibility of ATP interacting with noncanonical domains elsewhere in the receptor. Consistent with this idea, ATP has been shown to bind the carboxyl termini of certain members of the inward rectifier potassium channel (Kir) family and regulate channel function. Specifically, the Kir1.1, Kir6.1, and Kir6.2 channel-forming subunits of the K_{ATP} channel bind TNP-ATP with high affinity, although these proteins do not contain any known nucleotide-binding motifs (35). Extensive molecular modeling and mutagenesis strategies were employed to show that ATP binding occurs at an intermolecular interface between the amino terminus of one subunit of Kir6.2 and the carboxyl terminus of adjacent subunits (36–39). Similar approaches are needed to identify unknown additional ATP binding domains in $InsP_3R3$. Another possible strategy for identifying novel ATP binding domains could involve measuring 8-azido-[α-^{32}P]ATP binding to $InsP_3R3$-ΔATPB in the presence of $InsP_3$ and Ca^{2+} to initiate receptor activation, the rationale being that the conformational changes occurring during channel activation (40, 41) would reveal otherwise cryptic ATP binding sites. A further possibility is that ATP may exert its effects through an intermediary protein. In this scenario, any candidates must be tightly bound to the receptor, since ATP modulation of $InsP_3R3$ is readily evident in permeabilized cells.

ATP modulation of $InsP_3R2$ and $InsP_3R3$ is probably physiologically relevant in a number of cell types that express these isoforms. For example, in exocrine glands, these isoforms have been shown to be essential for Ca^{2+}-dependent exocytosis and fluid secretion (42), and thus ATP modulation of Ca^{2+} release might be expected to impact these processes. Also, given that multiple mammalian cell types express $InsP_3R2$ as the predominant isoform (43), ATP may exert modulatory effects on $InsP_3$-induced Ca^{2+} release in more physiological systems than previously appreciated. For instance, tissues such as liver, heart (43), salivary gland (44), and astrocytes (45) all express more $InsP_3R2$ relative to either $InsP_3R1$ or $InsP_3R3$. Furthermore, $InsP_3R2$ is expressed to some extent in a majority of cell types outside of the cerebellum, which expresses almost exclusively $InsP_3R1$ (43). Although ATP would probably affect $InsP_3$-induced Ca^{2+} release in these cells, the high sensitivity of $InsP_3R2$ to ATP would require cytosolic ATP levels to fall below 100 μM before adversely impacting signaling. Of note, ATP levels lower than 100 μM have been measured in ischemic brain tissue (46), suggesting that pathological periods of oxygen deprivation could result in a diminished $InsP_3R$ response even in cells expressing mostly $InsP_3R2$. Because $InsP_3R3$ has a lower sensitivity to ATP modulation, cells predominantly expressing this isoform might exhibit diminished $InsP_3R$ responses at much higher ATP levels. Pancreatic β-cells have been shown to express mostly $InsP_3R3$ (4) and experience metabolic fluctuations in cytosolic ATP levels that could impact the ability of $InsP_3$-raising agonists to modulate insulin secretion.

In summary, we have taken a mutagenic approach to address the contribution of the ATPB sites in the modulation of $InsP_3R2$ and $InsP_3R3$ by ATP. We found that the two isoforms differ in their sensitivity to ATP as well as the mechanisms by which ATP exerts its effects. The lower sensitivity of $InsP_3R3$ is probably bought about by a mechanism that does not require binding of ATP to the ATPB site. This situation may not, however, be unique to $InsP_3R3$. The sensitivity of $InsP_3R1$ to ATP has been determined in multiple systems to be higher than that of $InsP_3R3$, This enhanced sensitivity is thought to be brought about by a high affinity ATPA site unique to $InsP_3R1$, but it is possible that additional unknown ATP binding domains may also be present in $InsP_3R1$. Moreover, the contribution of the ATPB site in mediating the effects of ATP on $InsP_3R1$ has not been established. As reported in this study, mutation of the ATPB site in $InsP_3R2$ produced different results than mutation of the ATPB site in $InsP_3R3$. The sequences are highly similar in the regions surrounding these sites in all three $InsP_3R$ isoforms. It is therefore difficult to predict, based on sequence alone, what role the ATPB site in $InsP_3R1$ would play.

The present work adds to a growing body of evidence suggesting that ATP modulation of $InsP_3R$ is highly complex with isoform-dependent mechanisms. A complete understanding of these mechanisms will require additional mutagenesis and detailed functional analyses of defined receptor populations.

Acknowledgments—We thank Dr. T. Kurosaki for providing the DT40-KO cells, Dr. S. Joseph for providing the rat $InsP_3R3$ expression construct, and Lyndee Knowlton for excellent technical assistance.

REFERENCES

1. Patel, S., Joseph, S. K., and Thomas, A. P. (1999) *Cell Calcium* **25,** 247–264
2. Furuichi, T., Yoshikawa, S., Miyawaki, A., Wada, K., Maeda, N., and Mikoshiba, K. (1989) *Nature* **342,** 32–38
3. Sudhof, T. C., Newton, C. L., Archer, B. T., III, Ushkaryov, Y. A., and Mignery, G. A. (1991) *EMBO J.* **10,** 3199–3206
4. Blondel, O., Takeda, J., Janssen, H., Seino, S., and Bell, G. I. (1993) *J. Biol. Chem.* **268,** 11356–11363
5. Danoff, S. K., Ferris, C. D., Donath, C., Fischer, G. A., Munemitsu, S., Ullrich, A., Snyder, S. H., and Ross, C. A. (1991) *Proc. Natl. Acad. Sci. U. S. A.* **88,** 2951–2955
6. Iwai, M., Tateishi, Y., Hattori, M., Mizutani, A., Nakamura, T., Futatsugi, A., Inoue, T., Furuichi, T., Michikawa, T., and Mikoshiba, K. (2005) *J. Biol. Chem.* **280,** 10305–10317
7. Bezprozvanny, I. (2005) *Cell Calcium* **38,** 261–272
8. Foskett, J. K., White, C., Cheung, K. H., and Mak, D. O. (2007) *Physiol. Rev.* **87,** 593–658
9. Patterson, R. L., Boehning, D., and Snyder, S. H. (2004) *Annu. Rev. Biochem.* **73,** 437–465
10. Iino, M. (1991) *J. Gen. Physiol.* **98,** 681–698
11. Missiaen, L., Parys, J. B., Smedt, H. D., Sienaert, I., Sipma, H., Vanlingen, S., Maes, K., and Casteels, R. (1997) *Biochem. J.* **325,** 661–666
12. Maes, K., Missiaen, L., De Smet, P., Vanlingen, S., Callewaert, G., Parys, J. B., and De Smedt, H. (2000) *Cell Calcium* **27,** 257–267
13. Miyakawa, T., Maeda, A., Yamazawa, T., Hirose, K., Kurosaki, T., and Iino, M. (1999) *EMBO J.* **18,** 1303–1308
14. Bezprozvanny, I., and Ehrlich, B. E. (1993) *Neuron* **10,** 1175–1184
15. Tu, H., Wang, Z., Nosyreva, E., De Smedt, H., and Bezprozvanny, I. (2005) *Biophys. J.* **88,** 1046–1055
16. Mak, D. O., McBride, S., and Foskett, J. K. (1999) *J. Biol. Chem.* **274,** 22231–22237
17. Mak, D. O., McBride, S., and Foskett, J. K. (2001) *J. Gen. Physiol.* **117,** 447–456
18. Maes, K., Missiaen, L., Parys, J. B., Sienaert, I., Bultynck, G., Zizi, M., De Smet, P., Casteels, R., and De Smedt, H. (1999) *Cell Calcium* **25,** 143–152
19. Wierenga, R. K., and Hol, W. G. (1983) *Nature* **302,** 842–844
20. Tu, H., Miyakawa, T., Wang, Z., Glouchankova, L., Iino, M., and Bezprozvanny, I. (2002) *Biophys. J.* **82,** 1995–2004
21. Wagner, L. E., 2nd, Betzenhauser, M. J., and Yule, D. I. (2006) *J. Biol. Chem.* **281,** 17410–17419
22. Sugawara, H., Kurosaki, M., Takata, M., and Kurosaki, T. (1997) *EMBO J.* **16,** 3078–3088
23. Boehning, D., and Joseph, S. K. (2000) *J. Biol. Chem.* **275,** 21492–21499
24. Wang, W., and Malcolm, B. A. (2002) *Methods Mol. Biol.* **182,** 37–43
25. Dellis, O., Dedos, S. G., Tovey, S. C., Taufiq Ur, R., Dubel, S. J., and Taylor, C. W. (2006) *Science* **313,** 229–233
26. Dellis, O., Rossi, A. M., Dedos, S. G., and Taylor, C. W. (2008) *J. Biol. Chem.* **283,** 751–755
27. Uchida, K., Miyauchi, H., Furuichi, T., Michikawa, T., and Mikoshiba, K. (2003) *J. Biol. Chem.* **278,** 16551–16560
28. Maes, K., Missiaen, L., Parys, J. B., De Smet, P., Sienaert, I., Waelkens, E., Callewaert, G., and De Smedt, H. (2001) *J. Biol. Chem.* **276,** 3492–3497
29. Hiratsuka, T. (2003) *Eur. J. Biochem.* **270,** 3479–3485
30. Schug, Z. T., da Fonseca, P. C., Bhanumathy, C. D., Wagner, L., II, Zhang, X., Bailey, B., Morris, E. P., Yule, D. I., and Joseph, S. K. (2008) *J. Biol. Chem.* **283,** 2939–2948
31. Wagner, L. E., 2nd, Li, W. H., Joseph, S. K., and Yule, D. I. (2004) *J. Biol. Chem.* **279,** 46242–46252
32. Takata, M., Homma, Y., and Kurosaki, T. (1995) *J. Exp. Med.* **182,** 907–914
33. Li, C., Wang, X., Vais, H., Thompson, C. B., Foskett, J. K., and White, C. (2007) *Proc. Natl. Acad. Sci. U. S. A.* **104,** 12565–12570
34. Ignoul, S., and Eggermont, J. (2005) *Am. J. Physiol.* **289,** C1369–C1378
35. Vanoye, C. G., MacGregor, G. G., Dong, K., Tang, L., Buschmann, A. S., Hall, A. E., Lu, M., Giebisch, G., and Hebert, S. C. (2002) *J. Biol. Chem.* **277,** 23260–23270
36. Dong, K., Tang, L. Q., MacGregor, G. G., Leng, Q., and Hebert, S. C. (2005) *EMBO J.* **24,** 1318–1329
37. Trapp, S., Haider, S., Jones, P., Sansom, M. S., and Ashcroft, F. M. (2003) *EMBO J.* **22,** 2903–2912
38. Antcliff, J. F., Haider, S., Proks, P., Sansom, M. S., and Ashcroft, F. M. (2005) *EMBO J.* **24,** 229–239
39. Tucker, S. J., Gribble, F. M., Proks, P., Trapp, S., Ryder, T. J., Haug, T., Reimann, F., and Ashcroft, F. M. (1998) *EMBO J.* **17,** 3290–3296
40. Hamada, K., Miyata, T., Mayanagi, K., Hirota, J., and Mikoshiba, K. (2002) *J. Biol. Chem.* **277,** 21115–21118
41. Hamada, K., Terauchi, A., and Mikoshiba, K. (2003) *J. Biol. Chem.* **278,** 52881–52889
42. Futatsugi, A., Nakamura, T., Yamada, M. K., Ebisui, E., Nakamura, K., Uchida, K., Kitaguchi, T., Takahashi-Iwanaga, H., Noda, T., Aruga, J., and Mikoshiba, K. (2005) *Science* **309,** 2232–2234
43. Wojcikiewicz, R. J. (1995) *J. Biol. Chem.* **270,** 11678–11683
44. Zhang, X., Wen, J., Bidasee, K. R., Besch, H. R., Jr., Wojcikiewicz, R. J., Lee, B., and Rubin, R. P. (1999) *Biochem. J.* **340,** 519–527
45. Holtzclaw, L. A., Pandhit, S., Bare, D. J., Mignery, G. A., and Russell, J. T. (2002) *Glia* **39,** 69–84
46. Abe, K., Kogure, K., Yamamoto, H., Imazawa, M., and Miyamoto, K. (1987) *J. Neurochem.* **48,** 503–509